

Finite Element Analysis of Chemical Reaction Effect on Non-Darcy Convective Mixed Convective Double Diffusive Heat Transfer Flow Through a Porous Medium in Vertical Channel with Constant Heat Sources

B. Uma Devi¹, G. Sreenivas², R. Bhuvana Vijaya³ and D. R. V. Prasada Rao^{3&4}

¹Department of Mathematics, SBIT, Khammam, A.P., India

²Department of Mathematics, Gurunanak Engineering College, Ibrahim Patnam, Hyderabad, A.P., India

³Department of Mathematics, J.N.T.U.A. Anantapur – 515 002, A.P., India

⁴Department of Mathematics, S.K. University, Anantapur, A.P., India

ABSTRACT

We analyse the effect of chemical reaction on non-Darcy convective Heat and Mass transfer flow of a viscous electrically conducting fluid through a porous medium in a vertical channel with constant heat sources. The governing equations flow, heat and mass transfer are solved by using Galerkin finite element technique with quadratic polynomial approximations. The approximation solution is written directly as a linear combination of approximation functions with unknown nodal values as coefficients. Secondly, the approximation polynomials are chosen exclusively from the lower order piecewise polynomials restricted to contiguous elements. The velocity, temperature, concentration, shear stress and rate of Heat and Mass transfer are evaluated numerically for different values of $G, M, D^{-1}, N, Sc, \gamma$ and α

Keywords: Chemical Reaction, Heat and Mass Transfer, Porous Medium, Finite Element Analysis

INTRODUCTION

Non – Darcy effects on natural convection in porous media have received a great deal of attention in recent years because of the experiments conducted with several combinations of solids and fluids covering wide ranges of governing parameters which indicate that the experimental data for systems other than glass water at low Rayleigh numbers, do not agree with theoretical predictions based on the Darcy flow model. This divergence in the heat transfer results has been reviewed in detail in Cheng [5] among others. Extensive effects are thus being made to include the inertia and viscous diffusion terms in the flow equations and to examine their effects in order to develop a reasonable accurate mathematical model for convective transport in porous media. The work of Vafai and Tien [29] was one of the early attempts to account for the boundary and inertia effects in the momentum equation for a porous medium. They found that the momentum boundary layer thickness is of order of $\sqrt{\frac{k}{\epsilon}}$. Vafai and Thiyagaraja [30] presented analytical solutions for the velocity and temperature fields for the interface region using the Brinkman Forchheimer –extended Darcy equation. Detailed accounts of the recent efforts on non-Darcy convection have been recently reported in Tien and Hong [6], Cheng [5] and Kladias and Prasad [10]. Here, we will restrict our discussion to the vertical cavity only. Poulikakos and Bejan [17] investigated the inertia effects through the inclusion of Forchheimer's velocity squared term, and presented the boundary layer analysis for tall cavities. They also obtained numerical results for a few cases in order to verify the accuracy of their boundary layer analysis

for tall cavities. They also obtained numerical results for a few cases in order to verify the accuracy of their boundary layer solutions. This result in reversal of flow regimes from boundary layer to asymptotic to conduction as the contribution of the inertia term increases in comparison with that of the boundary term. They also reported a criterion for the Darcy flow limit.

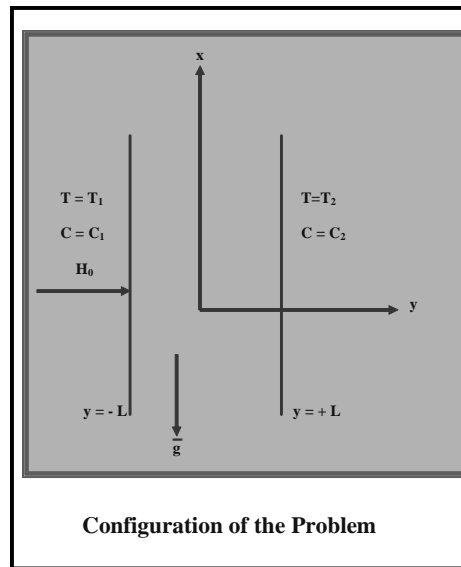
The Brinkman – Extended – Darcy modal was considered in Tong and Subramanian [28] to examine the boundary effects on free convection in a vertical cavity. While Tong and Subramanian performed a Weber – type boundary layer analysis, it was shown that for a fixed modified Rayleigh number, Ra , the Nusselt number; decrease with an increase in the Darcy number; the reduction being larger at higher values of Ra . A scale analysis as well as the computational data also showed that the transport term $(v \cdot \nabla)v$, is of low order of magnitude compared to the diffusion plus buoyancy terms. A numerical study based on the Forchheimer-Brinkman-Extended Darcy equation of motion has also been reported recently by Beckerman et al [4]. They demonstrated that the inclusion of both the inertia and boundary effects is important for convection in a rectangular packed – sphere cavity. Ruksana Begum et al [24] have discussed non-darcy convective heat transfer flow through a vertical channel with constant heat flux.

Also in all the above studies the thermal diffusion effect (known as Soret effect) has been neglected. This assumption is true when the concentration level is very low. Therefore, so ever, exceptions. The thermal diffusion effects for instance, has been utilized for isotropic separation and in mixtures between gases with very light molecular weight (H_2, He) and the medium molecular weight (N_2, air) the diffusion – thermo effects was found to be of a magnitude just it can not be neglected. In view of the importance of this diffusion – thermo effect, recently Jha and singh [8] studied the free convection and mass transfer flow in an infinite vertical plate moving impulsively in its own plane taking into account the Soret effect. Kafousias [9] studied the MHD free convection and mass transfer flow taking into account Soret effect. The analytical studies of Jha and singh and Kafousias [8,9] were based on Laplace transform technique. Abdul Sattar and Alam [1] have considered an unsteady convection and mass transfer flow of viscous incompressible and electrically conducting fluid past a moving infinite vertical porous plate taking into the thermal diffusion effects. Similarity equations of the momentum energy and concentration equations are derived by introducing a time dependent length scale. Malsetty et al [15] have studied the effect of both the soret coefficient and Dufour coefficient on the double diffusive convective with compensating horizontal thermal and solutal gradients. Balasubramanyam et al [3] have discussed the effect of heat generating heat sources on the non-darcy convective heat and mass transfer flow of a viscous fluid in a vertical channel. Sudarsana Reddy et al [26] have analysed the soret and Dufour effect on the non-darcy convective heat and mass transfer flow of a viscous fluid through a porous medium in a circular annulus in the presence of temperature gradient heat sources.

In this paper, we investigate effect of chemical reaction and thermo-diffusion on non-Darcy convective heat and Mass transfer flow of a viscous electrically conducting fluid through a porous medium in a vertical channel in the presence of constant heat source. The equations governing the flow, heat and mass transfer are solved by using Galerkin finite element technique with quadratic polynomial approximations. The approximation solution is written directly as a linear combination of approximation functions with unknown nodal values as coefficients. Secondly, the approximation polynomials are chosen exclusively from the lower order piecewise polynomials restricted to contiguous elements. The velocity, temperature, concentration, shear stress and rate of Heat and Mass transfer are evaluated numerically for different variations of parameter

FORMULATION OF THE PROBLEM

Consider a fully developed laminar mixed convective heat and mass transfer flow of a viscous, electrically conducting fluid through a porous medium in a vertical channel bounded by flat walls. We choose a Cartesian coordinate system $O(x,y,z)$ with x - axis in the vertical direction and y -axis normal to the walls. The walls are taken at $y = \pm L$. The walls are maintained at constant temperature and concentration. The temperature gradient in the flow field is sufficient to cause natural convection in the flow field. A constant axial pressure gradient is also imposed so that this resultant flow is a mixed convection flow. The porous medium is assumed to be isotropic and homogeneous with constant porosity and effective thermal diffusivity. The thermo physical properties of porous matrix are also assumed to be constant and Boussinesq approximation is invoked by confining the density variation to the buoyancy term. In the absence of any extraneous force flow is unidirectional along the x -axis which is assumed to be infinite.



The Brinkman-Forchheimer-extended Darcy equation which account for boundary inertia effects in the momentum equation is used to obtain the velocity field. Based on the above assumptions the governing equations are

$$-\frac{\partial p}{\partial x} + \left(\frac{\mu}{\delta}\right) \frac{\partial^2 u}{\partial y^2} - \left(\frac{\mu}{k}\right)u - (\sigma\mu_e^2 H_o^2)u - \frac{\rho\delta F}{\sqrt{k}} u^2 + \beta g(T - T_0) + \beta^* g(C - C_0) = 0 \tag{1}$$

$$\rho_0 C_p u \frac{\partial T}{\partial x} = k_f \frac{\partial^2 T}{\partial y^2} + Q \tag{2}$$

$$u \frac{\partial C}{\partial x} = D_1 \frac{\partial^2 C}{\partial y^2} - K'(C - C_0) + k_{11} \frac{\partial^2 T}{\partial y^2} \tag{3}$$

The boundary conditions are

$$\begin{aligned} u = 0, \quad T = T_1, \quad C = C_1 \quad \text{on } y = -L \\ u = 0, \quad T = T_2, \quad C = C_2 \quad \text{on } y = +L \end{aligned} \tag{4}$$

The axial temperature and concentration gradients $\frac{\partial T}{\partial x}$ & $\frac{\partial C}{\partial x}$ are assumed to be constant, say, A & B respectively where u is the velocity, T, C are the temperature and Concentration, p is the pressure, ρ is the density of the fluid, Cp is the specific heat at constant pressure, μ is the coefficient of viscosity, k is the permeability of the porous medium, δ is the porosity of the medium, β is the coefficient of thermal expansion, kf is the coefficient of thermal conductivity, F is a function that depends on the Reynolds number and the microstructure of porous medium, H is the magnetic field vector, σ is the electrical conductivity of the fluid, μ is the magnetic permeability of the medium, β* is the volumetric coefficient of expansion with mass fraction concentration and D1 is the chemical molecular diffusivity, K is the chemical reaction coefficient and Q is the strength of the heat source, k11 is the cross diffusivity. Here, the thermo physical properties of the solid and fluid have been assumed to be constant except for the density variation in the body force term (Boussinesq approximation) and the solid particles and the fluid are considered to be in the thermal equilibrium).

We define the following non-dimensional variables as

$$u' = \frac{u}{(v/L)}, (x', y') = (x, y)/L, p' = \frac{p\delta}{(\rho v^2/L^2)} \tag{5}$$

$$\theta = \frac{T-T_2}{T_1-T_2}, C' = \frac{C-C_2}{C_1-C_2}$$

Introducing these non-dimensional variables the governing equations in the dimensionless form reduce to (on dropping the dashes)

$$\frac{d^2u}{dy^2} = \pi + \delta(D^{-1} + M^2)u + \delta^2 \Delta u^2 - \delta G(\theta + NC) \tag{6}$$

$$\frac{d^2\theta}{dy^2} + \alpha = (PN_T)u \tag{7}$$

$$\frac{d^2C}{dy^2} - \gamma C = (Sc N_c)u - \frac{ScS_0}{N} \frac{d^2\theta}{dy^2} \tag{8}$$

where

$$\Delta = FD^{-1/2} \quad (\text{Inertia or Fochhemeir parameter})$$

$$G = \frac{\beta g(T_1 - T_2)L^3}{v^2} \quad (\text{Grashof Number})$$

$$D^{-1} = \frac{L^2}{k} \quad (\text{Darcy parameter})$$

$$Sc = \frac{v}{D_1} \quad (\text{Schmidt number})$$

$$M^2 = \frac{\sigma \mu_e^2 H_o^2 L^2}{v^2} \quad (\text{Hartmann Number})$$

$$N = \frac{\beta^* (C_1 - C_2)}{\beta(T_1 - T_2)} \quad (\text{Buoyancy ratio})$$

$$P = \frac{\mu C_p}{\lambda} \quad (\text{Prandtl Number})$$

$$\alpha = \frac{QL^2}{(T_1 - T_2)k_f} \quad (\text{Heat source parameter})$$

$$\gamma = \frac{K' L^2}{D_1} \quad (\text{Chemical reaction parameter})$$

$$N_T = \frac{AL}{(T_1 - T_2)} \quad (\text{Temperature gradient})$$

$$N_c = \frac{BL}{(C_1 - C_2)} \quad (\text{Concentration gradient})$$

$$S_0 = \frac{k_{11}\beta^*}{\beta v} \quad (\text{Soret parameter})$$

The corresponding boundary conditions are

$$u = 0, \theta = 1, C = 1 \text{ on } y = -1 \quad u = 0, \theta = 0, C = 0 \text{ on } y = +1 \tag{9}$$

FINITE ELEMENT ANALYSIS

To solve these differential equations with the corresponding boundary conditions, we assume if u^i, θ^i, c^i are the approximations of u, θ and C we define the errors (residual) E_u^i, E_θ^i, E_c^i as

$$E_u^i = \frac{d}{d\eta} \left(\frac{du^i}{d\eta} \right) - \delta(D^{-1} + M^2)u^i + \delta^2 \Delta (u^i)^2 - \delta G(\theta^i + NC^i) \tag{10}$$

$$E_c^i = \frac{d}{dy} \left(\frac{dC^i}{dy} \right) - \gamma C^i - ScN_c u^i - \frac{ScS_0}{N} \frac{d}{dy} \left(\frac{d\theta^i}{dy} \right) \tag{11}$$

$$E_\theta^i = \frac{d}{dy} \left(\frac{d\theta^i}{dy} \right) + \alpha - PN_T u^i \tag{12}$$

where

$$u^i = \sum_{k=1}^3 u_k \psi_k \quad C^i = \sum_{k=1}^3 C_k \psi_k \quad \theta^i = \sum_{k=1}^3 \theta_k \psi_k \quad \left. \right\} \quad (13)$$

These errors are orthogonal to the weight function over the domain of e^i under Galerkin finite element technique we choose the approximation functions as the weight function. Multiply both sides of the equations (10 – 12) by the weight function i.e. each of the approximation function ψ_j^i and integrate over the typical three noded linear element (η_e, η_{e+1}) we obtain

$$\int_{\eta_e}^{\eta_{e+1}} E_u^i \psi_j^i dy = 0 \quad (i = 1,2,3,4,) \quad (14)$$

$$\int_{\eta_e}^{\eta_{e+1}} E_c^i \psi_j^i dy = 0 \quad (i = 1,2,3,4,) \quad (15)$$

$$\int_{\eta_e}^{\eta_{e+1}} E_\theta^i \psi_j^i dy = 0 \quad (i = 1,2,3,4,) \quad (16)$$

where

$$\int_{\eta_e}^{\eta_{e+1}} \left(\frac{d}{d\eta} \left(\frac{du^i}{d\eta} \right) - \delta M_1^2 u^i + \delta^2 \Delta (u^i)^2 - \delta G (\theta^i + NC^i) \right) \psi_j^i dy = 0 \quad (17)$$

$$\int_{\eta_e}^{\eta_{e+1}} \left(\frac{d}{dy} \left(\frac{dC^i}{dy} \right) - \gamma C^i - Sc N_c u^i \right) \psi_j^i dy + \frac{Sc S_0}{N} \int_{\eta_e}^{\eta_{e+1}} \left(\frac{d}{dy} \left(\frac{d\theta^i}{dy} \right) \right) dy = 0 \quad (18)$$

$$\int_{\eta_e}^{\eta_{e+1}} \left(\frac{d}{dy} \left(\frac{d\theta^i}{dy} \right) + \alpha - PN_T u^i \right) \psi_j^i d\eta = 0 \quad (19)$$

Following the Galerkin weighted residual method and integration by parts method to the equations (17) – (19) we obtain

$$\left. \begin{aligned} \int_{\eta_e}^{\eta_{e+1}} \frac{d\Psi_j^i}{dy} \frac{d\psi^i}{dy} dy - \delta M_1^2 \int_{\eta_e}^{\eta_{e+1}} u^i \Psi_j^i dy + \delta^2 \Delta \int_{\eta_e}^{\eta_{e+1}} (u^i)^2 \Psi_j^i dy - \\ - \delta G \int_{\eta_e}^{\eta_{e+1}} (\theta^i + NC^i) \Psi_j^i dy = Q_{1,j} + Q_{2,j} \end{aligned} \right| \quad (20)$$

where – $Q_{1,j} = \Psi_j(\eta_e) \frac{du^i}{d\eta}(\eta_e)$

$Q_{2,j} = \Psi_j(\eta_{e+1}) \frac{du^i}{d\eta}(\eta_{e+1})$

$$\int_{\eta_e}^{\eta_{e+1}} \frac{d\Psi_j^i}{dy} \left(\frac{dC^i}{dy} \right) dy - \gamma \int_{\eta_e}^{\eta_{e+1}} C^i \psi_j^i d\eta + \frac{Sc S_0}{N} \int_{\eta_e}^{\eta_{e+1}} \frac{d\Psi_j^i}{dy} \left(\frac{d\theta^i}{dy} \right) dy - Sc N_c \int_{\eta_e}^{\eta_{e+1}} u^i \psi_j^i d\eta = R_{1,j} + R_{2,j} \quad (21)$$

where – $R_{1,j} = \Psi_j(\eta_e) \frac{dC^i}{dy}(\eta_e)$

$$R_{2,j} = \Psi_j(\eta_{e+1}) \frac{dC^i}{dy}(\eta_{e+1})$$

$$\int_{\eta_e}^{\eta_{e+1}} \frac{d\Psi_j^i}{dy} \frac{d\theta^i}{dy} dy - PN_T \int_{\eta_e}^{\eta_{e+1}} u^i \psi_j^i d\eta + \alpha \int_{\eta_e}^{\eta_{e+1}} \psi_j^i d\eta = S_{1,j} + S_{2,j} \tag{22}$$

where $S_{1,j} = \Psi_j(\eta_e) \frac{d\theta^i}{dy}(\eta_e)$

$$S_{2,j} = \Psi_j(\eta_{e+1}) \frac{d\theta^i}{dy}(\eta_{e+1})$$

Making use of equations (3.4) we can write above equations as

$$\sum_{k=1}^3 u_k \int_{\eta_e}^{\eta_{e+1}} \frac{d\psi_j^i}{dy} \frac{d\psi_k}{dy} dy - \sum_{k=1}^3 \delta M_1^2 u_k \int_{\eta_e}^{\eta_{e+1}} \psi_j^i \psi_k dy - \delta G \left(\sum_{k=1}^3 \theta_k \int_{\eta_e}^{\eta_{e+1}} \psi_j^i \psi_k dy + NC_k \sum_{k=1}^3 \psi_j^i \psi_k dy + \delta^2 \Delta \sum_{k=1}^3 u_k^2 \int_{\eta_e}^{\eta_{e+1}} \left(\frac{d\psi_k}{d\eta} \right)^2 \psi_j^i d\eta \right) = Q_{1,j} + Q_{2,j} \tag{23}$$

$$\sum_{k=1}^3 C_k \int_{\eta_e}^{\eta_{e+1}} \frac{d\psi_j^i}{dy} \frac{d\psi_k}{dy} dy - \gamma \sum_{k=1}^3 C_k \int_{\eta_e}^{\eta_{e+1}} \psi_j^i \psi_k d\eta + \frac{ScS_0}{N} \sum_{k=1}^3 \theta_k \int_{\eta_e}^{\eta_{e+1}} \frac{d\psi_j^i}{dy} \frac{d\psi_k}{dy} dy - ScN_c \sum_{k=1}^3 C_k \int_{\eta_e}^{\eta_{e+1}} \psi_j^i \psi_k dy = R_{1,j} + R_{2,j} \tag{24}$$

$$\sum_{k=1}^3 \theta_k \int_{\eta_e}^{\eta_{e+1}} \frac{d\psi_j^i}{dy} \frac{d\psi_k}{dy} dy + \alpha \sum_{k=1}^3 \int_{\eta_e}^{\eta_{e+1}} \psi_j^i dy - PN_T \sum_{k=1}^3 u_k \int_{\eta_e}^{\eta_{e+1}} \psi_k \psi_j^i dy = S_{1,j} + S_{2,j} \tag{25}$$

choosing different Ψ_j^i 's corresponding to each element η_e in the equation (20) yields a local stiffness matrix of order 3x3 in the form

$$(f_{i,j}^k)(u_i^k) - \delta G(g_{i,j}^k)(\theta_i^k + NC_i^k) + \delta M_1^2(m_{i,j}^k)(u_i^k) + \delta^2 \Delta(n_{i,j}^k)(u_{i,j}^k) = (Q_{i,j}^k) + (Q_{2,j}^k) \tag{26}$$

Likewise the equation (21) & (22) gives rise to stiffness matrices

$$(e_{i,j}^k)(C_i^k) - PN_C(m_{i,j}^k)(u_i^k) + \frac{ScS_0}{N}(l_{i,j}^k)(\theta_i^k) = R_{1,j}^k + R_{2,j}^k \tag{27}$$

$$(l_{i,j}^k)(\theta_i^k) - P_r N_T(t_{i,j}^k)(u_i^k) = S_{1,j}^k + S_{2,j}^k \tag{28}$$

where

$(f_{i,j}^k), (g_{i,j}^k), (m_{i,j}^k), (n_{i,j}^k), (e_{i,j}^k), (t_{i,j}^k), (l_{i,j}^k)$, are 3x3 matrices and $(Q_{2,j}^k), (Q_{1,j}^k), (R_{2,j}^k), (R_{1,j}^k), (S_{2,j}^k)$ and $(S_{1,j}^k)$ are 3x1 column matrices and such stiffness matrices (26) – (28) in terms of local nodes in each element are assembled using inter element continuity and equilibrium conditions to obtain the coupled global matrices in terms of the global nodal values of k, θ & C. In case we choose n-quadratic elements then the global matrices are of order 2n+1. The ultimate coupled global matrices are solved to determine the unknown global nodal values of the velocity, temperature and concentration in fluid region. In solving these global matrices an iteration procedure has been adopted to include the boundary and effects in the porous region.

The shape functions corresponding to

$$\begin{array}{lll}
 \Psi_1^1 = \frac{(y-4)(y-8)}{32} & \Psi_2^1 = \frac{(y-12)(y-16)}{32} & \Psi_3^1 = \frac{(y-20)(y-24)}{32} \\
 \Psi_1^2 = \frac{(y-2)(y-4)}{8} & \Psi_2^2 = \frac{(y-6)(y-8)}{8} & \Psi_3^2 = \frac{(y-10)(y-12)}{8} \\
 \Psi_1^3 = \frac{(3y-4)(3y-8)}{32} & \Psi_2^3 = \frac{(3y-12)(3y-16)}{32} & \Psi_3^3 = \frac{(3y-20)(3y-24)}{32} \\
 \Psi_1^4 = \frac{(y-1)(y-2)}{2} & \Psi_2^4 = \frac{(y-3)(y-4)}{2} & \Psi_3^4 = \frac{(y-5)(y-6)}{2} \\
 \Psi_1^5 = \frac{(5y-4)(5y-8)}{32} & \Psi_2^5 = \frac{(5y-12)(5y-16)}{32} & \Psi_3^5 = \frac{(5y-20)(5y-24)}{32}
 \end{array}$$

STIFFNESS MATRICES

The global matrix for θ is

$$A_3 X_3 = B_3 \tag{30}$$

The global matrix for C is

$$A_4 X_4 = B_4 \tag{31}$$

The global matrix u is

$$A_5 X_5 = B_5 \tag{32}$$

In fact, the non-linear term arises in the modified Brinkman linear momentum equation (20) of the porous medium. The iteration procedure in taking the global matrices is as follows. We split the square term into a product term and keeping one of them say u_i 's under integration, the other is expanded in terms of local nodal values as in (13), resulting in the corresponding coefficient matrix $(n_{i,j}^k)$'s in (26), whose coefficients involve the unknown u_i 's .

To evaluated (27) to begin with choose the initial global nodal values of u_i 's as zeros in the zeroth approximation. We evaluate u_i 's , θ_i 's and C_i 's in the usual procedure mentioned earlier. Later choosing these values of u_i 's as first order approximation calculate θ_i 's, C_i 's. In the second iteration, we substitute for u_i 's the first order approximation of and u_i 's and the first approximation of θ_i 's and C_i 's obtain second order approximation. This procedure is repeated till the consecutive values of u_i 's , θ_i 's and C_i 's differ by a preassigned percentage. For computational purpose we choose five elements in flow region.

**For M=0 the results are in good agreement with Leelakumari [16].*

**For So=0 the results are in good agreement with Balasubramanyam et al [3]*

RESULTS AND DISCUSSION

In this analysis we investigate the effect of chemical reaction and thermo diffusion on the non-Darcy convective Heat and mass transfer flow of a viscous fluid in a vertical channel in the presence of constant heat sources.

Figs. 1-6 represent the axial velocity with different variation of G, M, D^{-1} , α , Sc, S_0 , N and γ . Fig. 1 represents u with Grashof number G. It is found that the axial velocity is in the vertically downward direction for $G>0$ and is in the vertically upward direction for $G<0$. $|u|$ enhances with increase in $|G|$ with maximum at $y = 0.5$. The variation of u with M and D^{-1} is shown in fig. 2. It is found that lesser the permeability of the porous medium/higher the Lorentz force lesser $|u|$ in the entire fluid region. The magnitude of u experiences an enhancement with increase in the strength of the heat source/sink (fig.3). The variation of u with Schmidt number Sc shows that lesser the molecular diffusivity larger $|u|$ in the flow region (fig.4). We notice from fig.5 that $|u|$ enhances with increase in $S_0>0$ and reduces with $|S_0| (<0)$ (fig.6). The variation of u with buoyancy ratio N shows that when the molecular buoyancy force dominates over the thermal buoyancy force the magnitude of u reduces when the buoyancy forces act in the same direction and for the forces acting in opposite directions $|u|$ enhances in the fluid region (fig.6). The effect of

the chemical reaction parameter γ on u is shown in fig.7. It is found that $|u|$ reduces in the degenerating chemical reaction case and enhances in the generating chemical reaction case in the entire fluid region.

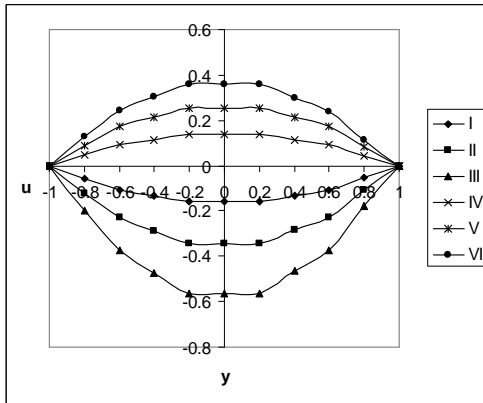


Fig. 1 : Variation of u with G

	I	II	III	IV	V	VI
G	10^2	3×10^2	5×10^2	-10^2	-3×10^2	-5×10^2

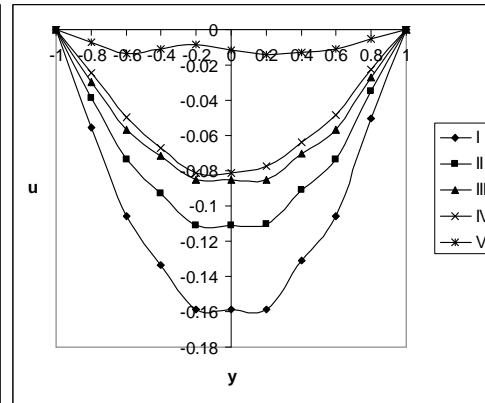


Fig. 2 : Variation of u with D^{-1} & M

	I	II	III	IV	V
D^{-1}	10^3	3×10^3	5×10^3	10^3	10^3
M	2	2	2	4	6

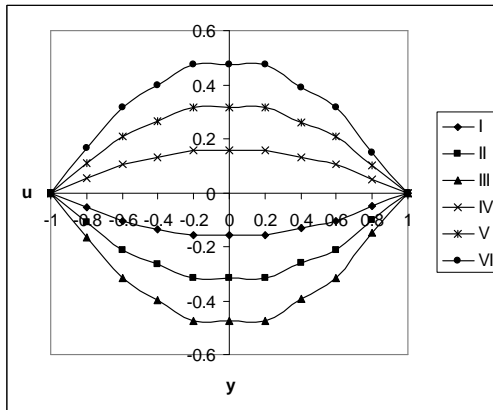


Fig. 3 : Variation of u with α

	I	II	III	IV	V	VI
α	2	4	6	-2	-4	-6

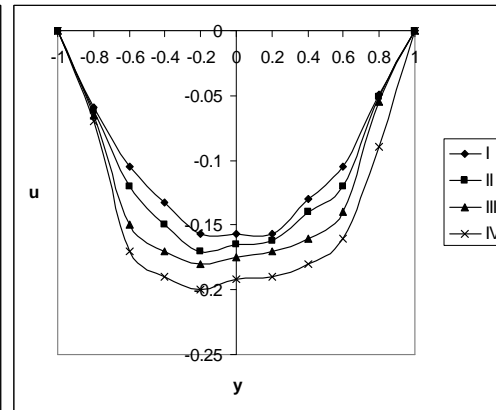


Fig. 4 : Variation of u with Sc

	I	II	III	IV
Sc	0.24	0.6	1.3	2.01

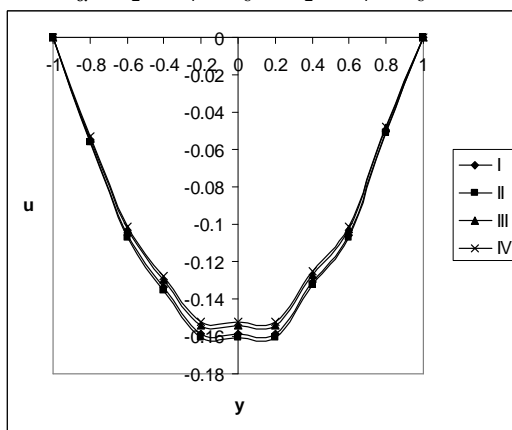


Fig. 5 : Variation of u with S_0

	I	II	III	IV
S_0	0.5	1	-0.5	-1.0

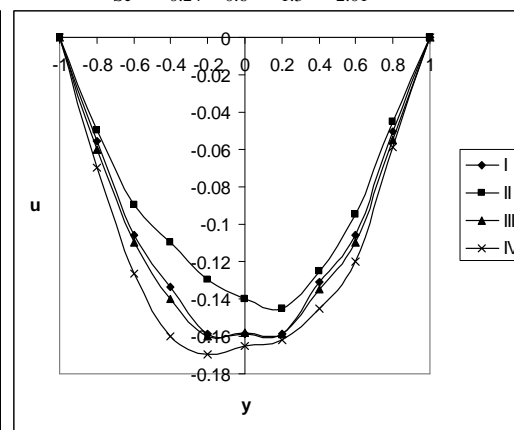


Fig. 6 : Variation of u with N

	I	II	III	IV
N	1	2	-0.5	-0.8

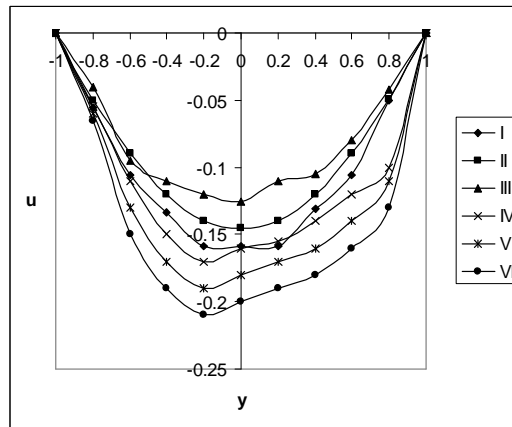


Fig. 7 : Variation of u with γ

	I	II	III	IV	V	VI
γ	0.5	1.5	2.5	-0.5	-1.5	-2.5

The non-dimensional temperature (θ) is shown in figs. 8-15 for different parametric values. Fig. 8 represents θ with Grashof number G. It is found that the actual temperature enhances in the heating case and depreciates in the cooling case with maximum attained at $y = -0.2$. The variation of θ with M and D^{-1} shows that lesser the permeability of the porous medium/higher the Lorentz force lesser the actual temperature in the entire flow region (figs. 9&10). Fig. 11 represents θ with heat source parameter α . It is found that the actual temperature enhances with increase in the strength of the heat source and reduces with heat sink (fig.11). Lesser the molecular diffusivity larger the actual temperature (fig.12). The actual temperature reduces with increase in S_0 (>0) and enhances with $|S_0|$ (<0)(fig.13). When the molecular buoyancy force dominates over the thermal buoyancy force the actual temperature reduces when the buoyancy forces act in the same direction and for the forces acting in opposite directions it enhances in the flow region (fig. 14). The variation of θ with chemical reaction parameter γ is shown in fig.5. It is found that the actual temperature reduces in the degenerating chemical reaction case and enhances in the generating chemical reaction case.

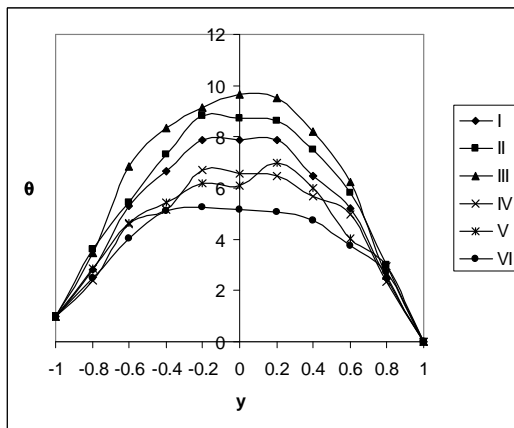


Fig. 8 : Variation of θ with G

	I	II	III	IV	V	VI
G	10^2	3×10^2	5×10^2	-10^2	-3×10^2	-5×10^2

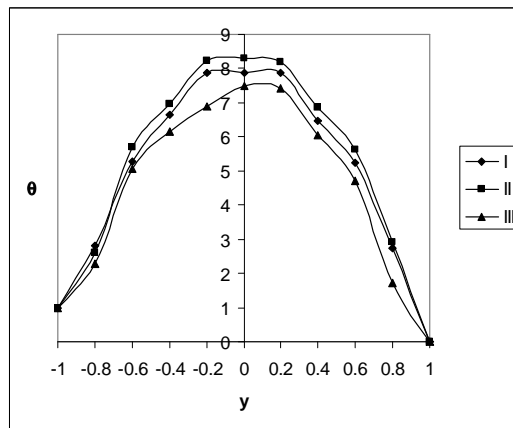


Fig. 9 : Variation of θ with D^{-1}

	I	II	III
D^{-1}	10^3	3×10^3	5×10^3

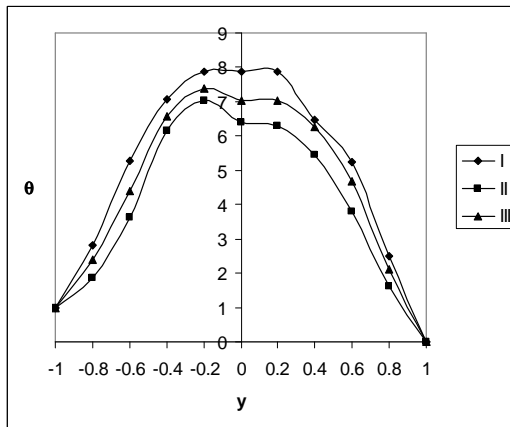


Fig. 10 : Variation of θ with α

I	II	III	
M	2	4	6

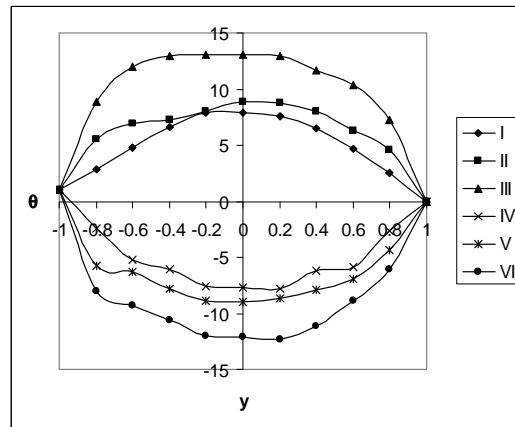


Fig. 11 : Variation of θ with α

I	II	III	IV	V	VI	
α	2	4	6	-2	-4	-6

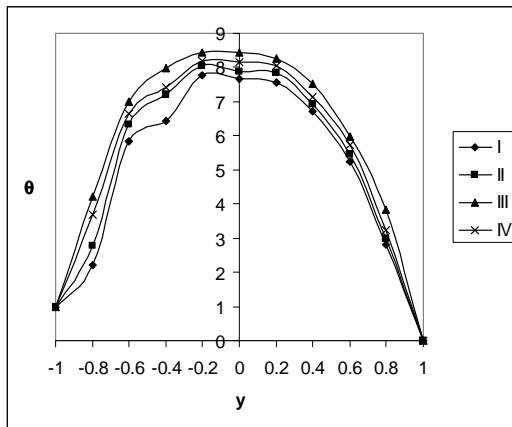


Fig. 12 : Variation of θ with Sc

I	II	III	IV	
Sc	0.24	0.6	1.3	2.01

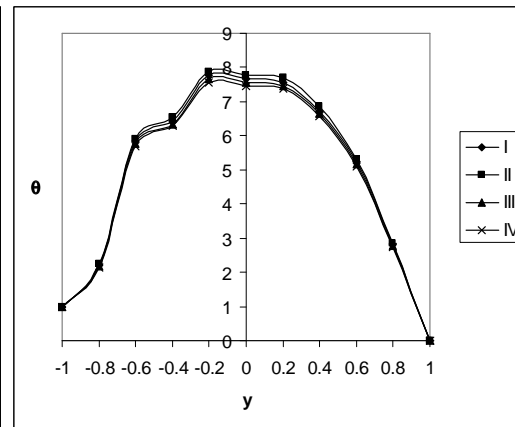


Fig. 13 : Variation of θ with S_0

I	II	III	IV	
S_0	0.5	1	-0.5	-1.0

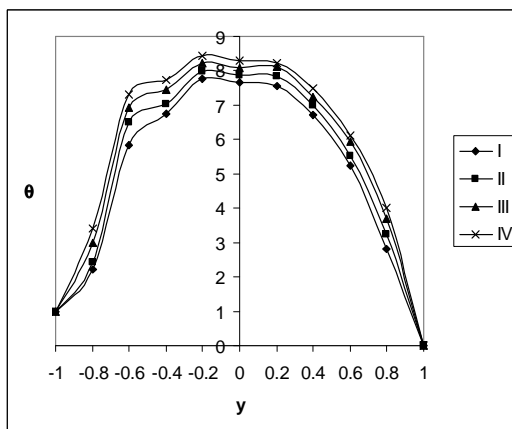


Fig. 14 : Variation of θ with N

I	II	III	IV	
N	1	2	-0.5	-0.8

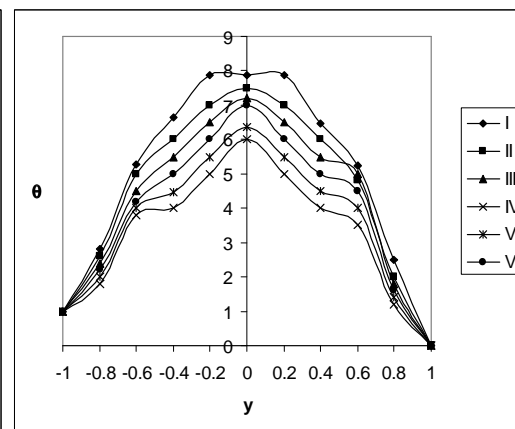


Fig. 15 : Variation of θ with γ

I	II	III	IV	V	VI	
γ	0.5	1.5	2.5	-0.5	-1.5	-2.5

The concentration distribution (C) is shown in figs.16-23 for different parametric values. Fig.16 represents C with Grashof number G. It is found that the actual concentration depreciates in the heating case and enhances in the

cooling case with maximum attained at $y = -0.4$ and the point of maximum shifts towards the left boundary with increase in $G > 0$ and for $G < 0$, it is attained at $y = -0.2$. The variation of C with M and D^{-1} shows that the actual concentration enhances with increase in M or D^{-1} (figs.17&18). The variation of C with α shows that the actual concentration enhances with increase in $\alpha > 0$ and depreciates with $|\alpha| (< 0)$ (fig. 19). Lesser the molecular diffusivity larger the actual concentration (fig.20). Also the actual concentration enhances with increase in $S_0 > 0$ and depreciates with $|S_0| (< 0)$ (fig.21). From fig.22 we find that the actual concentration depreciates when the buoyancy forces act in the same direction and for the forces acting in opposite directions it enhances in the entire flow region. The variation of C with γ shows that the actual concentration reduces in the degenerating chemical reaction and enhances in the generating case (fig. 23).

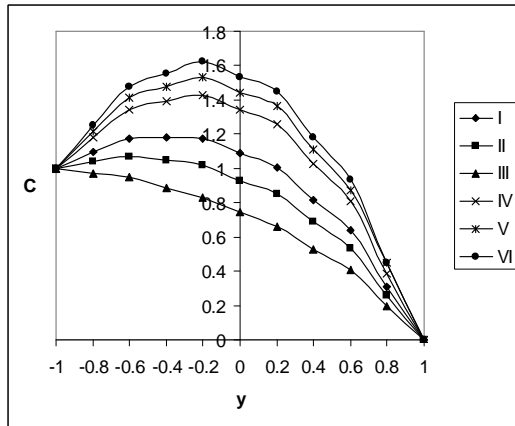


Fig. 16 : Variation of C with G
 I II III IV V VI
 G 10^2 3×10^2 5×10^2 -10^2 -3×10^2 -5×10^2

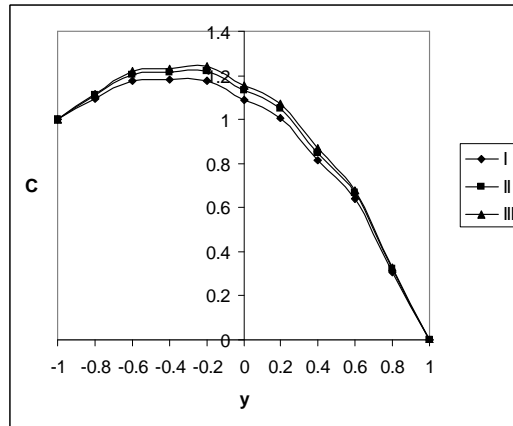


Fig. 17 : Variation of C with D^{-1}
 I II III
 D^{-1} 10^3 3×10^3 5×10^3

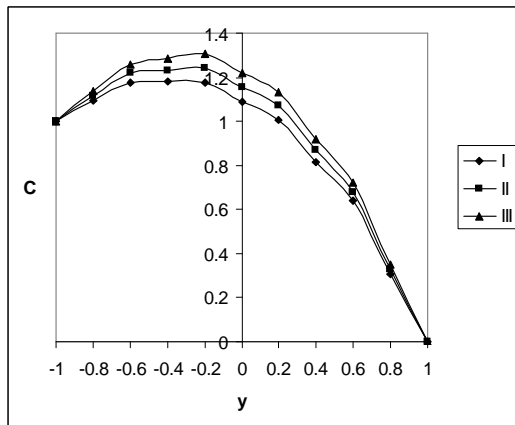


Fig. 18 : Variation of C with α
 I II III
 M 2 4 6

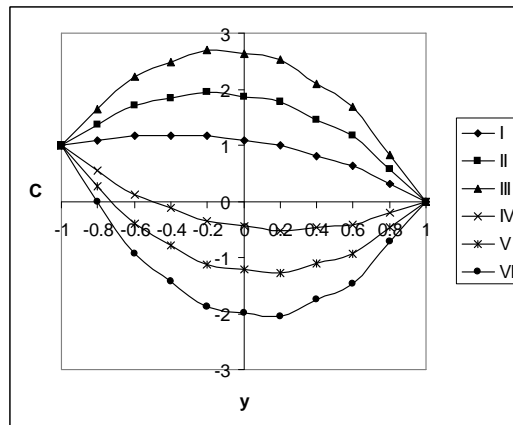


Fig. 19 : Variation of C with α
 I II III IV V VI
 α 2 4 6 -2 -4 -6

The rate of heat transfer (Nusselt number) at the walls $y = -1$ & 1 are shown in tables 1-6 for different parametric values. Tables 1&4 represent Nu with G , M , D^{-1} and α . It is found that the rate of heat transfer enhances with $G > 0$ and reduces with $G < 0$ at both the walls. Lesser the permeability of the porous medium smaller $|Nu|$ for $G > 0$ and larger for $G < 0$ at both the walls. The variation of Nu with Hartman number M shows that the rate of heat transfer at $y = -1$ reduces with M in the heating case and enhances in the cooling case while at $y = 1$, it enhances with M for all G . Also it experiences an enhancement with increase in the strength of the heat source/sink. The variation of Nu with buoyancy ratio N shows that the rate of the heat transfer reduces with N at $y = -1$ & 1 when the buoyancy forces act in the same direction and for the forces acting in opposite directions, $|Nu|$ enhances at $y = -1$ and reduces at $y = 1$. Lesser the molecular diffusivity larger $|Nu|$ for $G > 0$ and lesser for $G < 0$ at both the walls (tables 2&5). The variation of Nu with Soret parameter S_0 shows that it enhances for $G > 0$ and reduces for $G < 0$ with increase in $S_0 > 0$ at both the walls while for $S_0 < 0$, it reduces in the heating case and enhances in the cooling case at both the walls. Also the rate

of heat transfer enhances in the degenerating chemical reaction case for all G and in the generating reaction case, it enhances in the heating case and reduces in the cooling case at both the walls (tables 3&6).

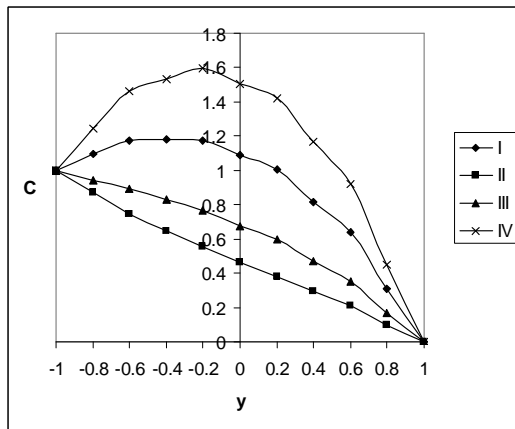


Fig. 20 : Variation of C with Sc
I II III IV
Sc 0.24 0.6 1.3 2.01

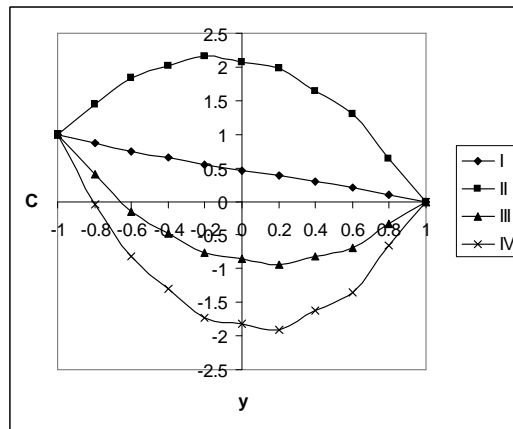


Fig. 21 : Variation of C with S₀
I II III IV
S₀ 0.5 1 -0.5 -1.0

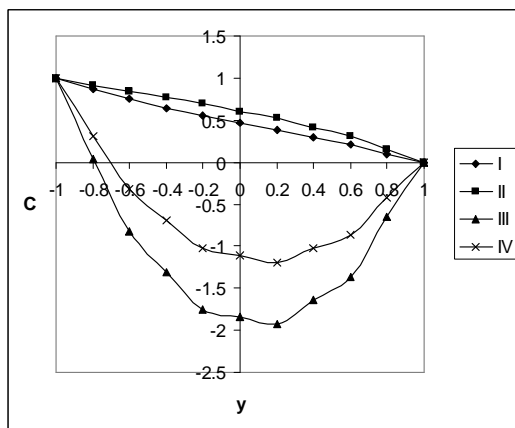


Fig. 22 : Variation of C with N
I II III IV
N 1 2 -0.5 -0.8

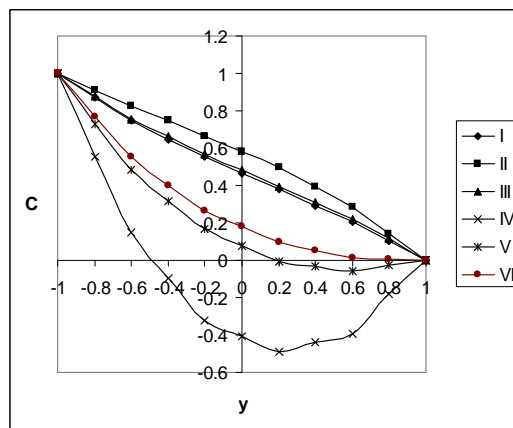


Fig. 23 : Variation of C with γ
I II III IV V VI
 γ 0.5 1.5 2.5 -0.5 -1.5 -2.5

Table.1 : Nusselt number Nu₁ at y=-1

G	I	II	III	IV	V	VI	VII	VIII	IX	X
10 ²	300.06	284.588	281.07	293.585	290.112	586.168	872.276	-272.15	-558.26	-844.37
3x10 ²	354.953	297.098	287.218	329.071	316.474	695.805	1036.66	-326.75	-667.6	-1008.4
-10 ²	260.034	272.867	275.971	265.085	267.975	506.225	752.417	-232.35	-478.54	-724.73
-3x10 ²	229.544	262.109	271.507	241.692	249.02	445.333	661.121	-202.03	-417.82	-633.61
M	2	4	6	2	2	2	2	2	2	2
D ⁻¹	10 ³	10 ³	10 ³	3x10 ³	5x10 ³	10 ³				
α	2	2	2	2	2	4	6	-2	-4	-6

Table-2 : Nusselt number Nu₁ at y=-1

G	I	II	III	IV	V	VI	VII
10 ²	300.06	229.99	300.16	300.17	299.87	299.94	300.19
3x10 ²	354.95	354.18	356.39	356.39	354.58	354.71	355.2
-10 ²	260.03	259.99	260.11	260.11	260.25	260.17	259.89
-3x10 ²	229.54	229.23	230.11	230.11	230.21	229.99	229.09
N	1	2	-0.5	-0.8	1	1	1
Sc	1.3	1.3	1.3	1.3	0.24	0.6	2.01

Table-3 : Nusselt number Nu_1 at $y=-1$

G	I	II	III	IV	V	VI	VII	VIII	IX
10^2	300.06	300.352	299.48	299.19	299.907	299.877	299.611	299.757	299.787
3×10^2	354.953	356.191	352.505	351.294	354.65	354.59	354.058	354.351	354.411
-10^2	260.034	259.818	260.468	260.685	260.209	260.243	260.545	260.379	260.346
-3×10^2	229.544	229.045	230.553	231.061	230.094	230.201	231.141	230.625	230.52
So	0.5	1	-0.5	-1	0.5	0.5	0.5	0.5	0.5
γ	0.5	0.5	0.5	0.5	1.5	2.5	-0.5	-1.5	-2.5

Table-4 : Nusselt number Nu_2 at $y=1$

G	I	II	III	IV	V	VI	VII	VIII	IX	X
10^2	4442.12	4203.98	4137.34	4342.09	4288.43	8866.74	13291.4	-4407.1	-8831.7	-13256
3×10^2	5290.22	4386.23	4281.26	4889.97	4723.99	10561.4	15832.5	-5252.1	-10523	-15794
-10^2	3823.75	4021.67	4070.37	3901.78	3946.44	7631.14	11438.5	-3791.1	-7598.4	-11405
-3×10^2	3352.71	3855.75	4036.78	3540.34	3653.6	6690.01	10027.3	-3321.7	-6658.9	-9996.2
M	2	4	6	2	2	2	2	2	2	2
D^{-1}	10^3	10^3	10^3	10^3	3×10^3	5×10^3	10^3	10^3	10^3	10^3
α	2	2	2	2	2	4	6	-2	-4	-6

Table-5 : Nusselt number Nu_2 at $y=1$

G	I	II	III	IV	V	VI	VII
10^2	4442.12	4441.17	4443.57	4443.86	4439.23	4440.21	4444.06
3×10^2	5290.22	5278.28	5308.6	5312.34	5284.45	5286.42	5294.06
-10^2	3823.75	3823.05	3824.8	3825.01	3827.06	3825.94	3821.54
-3×10^2	3352.71	3347.8	3360.09	3361.54	3363.1	3359.6	3345.8
N	1	2	-0.5	-0.8	1	1	1
Sc	1.3	1.3	1.3	1.3	0.24	0.6	2.01

Table-6 : Nusselt number Nu_2 at $y=1$

G	I	II	III	IV	V	VI	VII	VIII	IX
10^2	4442.12	4446.63	4433.15	4428.67	4439.28	4439.28	4435.16	4437.43	4437.89
3×10^2	5290.22	5309.35	5252.38	5233.66	5285.51	5284.57	5276.31	5280.87	5281.79
-10^2	3823.75	3820.41	3830.46	3833.82	3826.47	3827	3831.67	3829.11	3828.58
-3×10^2	3352.71	3345.03	3368.35	3376.2	3361.25	3362.92	3377.46	3369.48	3367.86
So	0.5	1	-0.5	-1	0.5	0.5	0.5	0.5	0.5
γ	0.5	0.5	0.5	0.5	1.5	2.5	-0.5	-1.5	-2.5

Table-7 : Sherwood number fu_1 at $y=-1$

G	I	II	III	IV	V	VI	VII	VIII	IX	X
10^2	15.9974	16.3558	16.4284	16.1471	16.2275	18.9102	21.823	10.1718	7.2589	4.3462
3×10^2	14.7286	16.0578	16.31	15.3263	15.6286	16.3761	18.0237	11.4335	9.7859	8.1384
-10^2	16.9236	16.6263	16.5553	16.8067	16.7397	20.76	24.5964	9.2508	5.4144	1.578
-3×10^2	17.6298	16.8755	16.6827	17.3483	17.1786	22.1703	26.7109	8.5486	4.0081	-0.5325
M	2	4	6	2	2	2	2	2	2	2
D^{-1}	10^3	10^3	10^3	3×10^3	5×10^3	10^3	10^3	10^3	10^3	10^3
α	2	2	2	2	2	4	6	-2	-4	-6

Table-8 : Sherwood number fu_1 at $y=1$

G	I	II	III	IV	V	VI	VII
10^2	15.9974	14.1586	4.9478	7.7086	13.6241	14.431	17.583
3×10^2	14.7286	12.5616	1.5167	4.8002	13.3907	13.8466	15.6169
-10^2	16.9236	15.3392	7.4052	9.7837	13.7934	14.8556	19.0247
-3×10^2	17.6298	16.2478	9.2526	11.3393	13.9218	15.1783	20.1276
N	1	2	-0.5	-0.8	1	1	1
Sc	1.3	1.3	1.3	1.3	0.24	0.6	2.01

The rate of mass transfer (Sherwood number) at the walls $y = -1$ & 1 are shown in tables 7-12 for different parametric values. It is found that the rate of mass transfer reduces at $y = -1$ and enhances at $y = 1$ with increase in $G > 0$ while a reversed effect is observed with $G < 0$. The variation of Sh with M & D^{-1} shows that lesser the permeability of the porous medium/higher the Lorentz forces larger $|Sh|$ at $y = -1$ and smaller at $y = +1$ for $G > 0$ and lesser at $y = -1$ and

larger at $y = 1$ for $G < 0$. With respect to heat source parameter α , we find that the rate of mass transfer enhances at $y = -1$ and reduces at $y = 1$ with increase in the strength of the heat source while an increase in the strength of the heat sink, reduces, $|Sh|$ at $y = -1$ and enhances at $y = 1$ for all G (tables 7&9). The variation of Sh with N shows that the rate of mass transfer depreciates at $y = -1$ and enhances at $y = 1$ with increase in $N > 0$ and it enhances at $y = -1$ and reduces at $y = 1$ with $|N|$ for all G . Also lesser the molecular diffusivity larger $|Sh|$ at $y = -1$ and lesser $|Sh|$ at $y = 1$ for all G . (tables 8&11). With respect to Soret parameter S_0 , we find that $|Sh|$ enhances at $y = -1$ and reduces at $y = 1$ with increase in $S_0 > 0$ and a reversed effect is noticed in the behaviour of $|Sh|$ with $|S_0| (< 0)$. The variation of Sh with chemical reaction parameter γ , we find that the rate of mass transfer reduces at $y = -1$ and enhances at $y = 1$ in the degenerating reaction case and in and reduces at $y = 1$ for all G (tables 9&12).

Table-9 : Sherwood number fu_1 at $y=-1$

G	I	II	III	IV	V	VI	VII	VIII	IX
10^2	15.9974	19.6756	8.6631	5.06703	14.0834	13.7333	10.3432	12.1771	12.5467
3×10^2	14.7286	19.0953	6.0883	1.81418	13.6672	13.4846	11.554	12.5869	12.7934
-10^2	16.9236	20.0973	10.559	7.3693	14.3856	13.9136	9.4735	11.8811	12.3684
-3×10^2	17.6298	20.4177	12.015	9.1885	14.615	14.0503	8.8183	11.6573	12.2335
S_0	0.5	1	-0.5	-1	0.5	0.5	0.5	0.5	0.5
γ	0.5	0.5	0.5	0.5	1.5	2.5	-0.5	-1.5	-2.5

Table-10 : Sherwood number fu_2 at $y=1$

G	I	II	III	IV	V	VI	VII	VIII	IX	X
10^2	12.0159	11.7241	11.6444	11.8934	11.8277	9.5396	7.0633	16.9685	19.4448	21.9211
3×10^2	13.054	11.9495	11.8189	12.5644	12.3619	11.6141	10.1743	15.9336	17.3735	18.8133
-10^2	11.2582	11.5009	11.5603	11.3539	11.4086	8.0253	4.7923	17.724	20.957	24.1899
-3×10^2	10.6805	11.2974	11.5143	10.9106	11.0495	6.8708	3.06104	18.3002	22.11	25.9197
M	2	4	6	2	2	2	2	2	2	2
D^{-1}	10^3	10^3	10^3	3×10^3	5×10^3	10^3	10^3	10^3	10^3	10^3
a	2	2	2	2	2	4	6	-2	-4	-6

Table-11 : Sherwood number fu_2 at $y=1$

G	I	II	III	IV	V	VI	VII
10^2	12.0159	13.5671	21.3373	19.0082	14.034	13.348	10.6673
3×10^2	13.054	14.8735	24.1447	21.3881	14.2251	13.8261	12.2757
-10^2	11.2582	12.6014	19.3267	17.3104	13.8955	13.0006	9.4881
-3×10^2	10.6805	11.8583	17.8154	16.0377	13.7905	12.7366	8.5862
N	1	2	-0.5	-0.8	1	1	1
Sc	1.3	1.3	1.3	1.3	0.24	0.6	2.01

Table-12 : Sherwood number fu_2 at $y=1$

G	I	II	III	IV	V	VI	VII	VIII	IX
10^2	12.0159	8.91286	18.2042	21.2895	13.5351	13.6987	16.6908	15.2031	14.9124
3×10^2	13.054	9.38754	20.3116	23.9033	13.8753	13.9009	15.7001	14.8677	14.7106
-10^2	11.2582	8.56797	16.6519	19.3554	13.2882	13.5525	17.4023	15.4452	15.0583
-3×10^2	10.6805	8.30594	15.4604	17.8658	13.1009	13.4419	17.9383	15.6283	15.1687
S_0	0.5	1	-0.5	-1	0.5	0.5	0.5	0.5	0.5
γ	0.5	0.5	0.5	0.5	1.5	2.5	-0.5	-1.5	-2.5

CONCLUSION

In this analysis we discuss the effect of thermo diffusion and chemical reaction effects on non-darcy convective heat and mass transfer flow in a vertical channel in the presence of heat sources. By using Galerkin finite element technique the equation are solved. The importance conclusions of this analysis are:

1. $|u|$ enhances with increase in $S_0 > 0$ and reduces with $|S_0| (< 0)$. $|u|$ reduces in the degenerating chemical reaction case and enhances in the generating chemical reaction case in the entire fluid region.
2. The actual temperature reduces with increase in $S_0 (> 0)$ and enhances with $|S_0| (< 0)$. The actual temperature reduces in the degenerating chemical reaction case and enhances in the generating chemical reaction case.
3. The actual concentration enhances with increase in $S_0 > 0$ and depreciates with $|S_0| (< 0)$. The actual concentration reduces in the degenerating chemical reaction and enhances in the generating case.

4. The Nusselt number enhances for $G > 0$ and reduces for $G < 0$ with increase in $S_0 > 0$ at both the walls while for $S_0 < 0$, it reduces in the heating case and enhances in the cooling case at both the walls. Also the rate of heat transfer enhances in the degenerating chemical reaction case for all G and in the generating reaction case, it enhances in the heating case and reduces in the cooling case at both the walls.
5. $|Sh|$ enhances at $y = -1$ and reduces at $y = 1$ with increase in $S_0 > 0$ and a reversed effect is noticed in the behaviour of $|Sh|$ with $|S_0| (< 0)$. The rate of mass transfer reduces at $y = -1$ and enhances at $y = 1$ in the degenerating reaction case and in and reduces at $y = 1$ for all G .

REFERENCES

- [1] Abdul Sattar Md and Alam Md, Thermal diffusion as well as transpiration effect on MHD free convection and Mass Transfer flow past an accelerated vertical porous plate, *Ind Journal of Pure and Applied Maths.* **1995**, 24, 679-688.
- [2] Ayani M B and Fsfahani JH, The effect of radiation on the natural convection induced by a line heat source, *Int.J.Numer.Method,Heat fluid flow*, (U.K.), **2006**, 16, 28-45.
- [3] Balasubramanyam M, Sudarsanan Reddy P and Prasada Rao, D.R.V., Non-darcy viscous electrically conducting heat and mass transfer flow through a porous medium in a vertical channel in the presence of heat generating sources., *Int.J.Appl.Mat and Mech*, **2010**, 6(15), 35-45.
- [4] Beckermann C, Visakanta R and Ramadhyani S, A numerical study of non-Darcian natural convection in a vertical enclosure filled with a porous medium, *Numerical Heat transfer*, **1986**, 10, 557-570.
- [5] Cheng P, Heat transfer in geothermal systems, *Adv.Heat transfer*, **1978**, 14, 1-105.
- [6] D Tien C V and Hong J T, Natural convection in porous media under non-Darcian and non-uniform permeability conditions, hemisphere, *Washington.C.* **1985**.
- [7] El Hakiem M.A, MHD oscillatory flow on free convection radiation through a porous medium with constant suction velocity, *J.mason.Mater.*, **2000**, 220, 271-276.
- [8] Jha B K and Singh A K, *Astrophys. Space Sci.* **1990**, 173, 251.
- [9] Kafousia N G, *Astrophys. Space Sci.*, **1990**, 173, 251.
- [10] Kalidas N and Prasad V, Benard convection in porous media Effects of Darcy and Prandtl Numbers, *Int. Syms. Convection in porous media*, non-Darcy effects, proc. 25th Nat. Heat Transfer Conf., **1988**, 1, 593-604.
- [11] Kavitha, A, Hemadri Reddy, R, Sreenadh, S, Saravana, R and Srinivas, A.N.S.: *Advances in Appl. Sci. Research*, **2011**, 2(1), 269-279.
- [12] Krishna kumara, S.V.H.N, Ravi Kumar, Y.V.K and Ramana Murthy, M.V.: *Advances in Appl. Sci. Research*, **2011**, 2(6), 439-453.
- [13] Kumar A, Singh N P, Singh A K, Kumar H, MHD free convection flow of a viscous fluid past a porous vertical plate through non-homogeneous porous medium with radiation and temperature gradient dependent heat source in slip flow regime, *Ultra Sci.Phys.Sci (India)*, **2006**, 18, 39-46.
- [14] Makinde O.D, Free convection flow with thermal radiation and mass transfer pass a moving vertical porous plate, *Int. Commun. Heat and Mass transfer (U.K)*, **2005**, 32, 1411-1419.
- [15] Malasetty M S, Gaikwad S N, Effect of cross diffusion on double diffusive convection in the presence of horizontal gradient, *Int.Journal Eng.Science*, **2002**, 40, 773-787.
- [16] Nagaleelakumari S, Effect of chemical reaction and thermo-diffusion on non-darcy convective heat and mass transfer flow of a viscous fluid through a porous medium in a vertical channel, *Ph.D. thesis, S.P.Mahila University, Tirupati*, **2012**.
- [17] Poulikakos D, and Bejan A, The Departure from Darcy flow in Nat. Convection in a vertical porous layer, *physics fluids*, **1985**, 28, 3477-3484.
- [18] Prasad V, and Tuntomo A, Inertia Effects on Natural Convection in a vertical porous cavity, *Numerical Heat Transfer*, **1987**, 11, 295-320.
- [19] Prasad V, Natural convection in porous media., *Ph.D thesis, S.K. University, Anantapur*, **1983**
- [20] Raghunatha Rao T and Prasada Rao D R V, The influence of heat transfer on peristaltic transport of a couple stress fluid through a porous medium, *Advances in Applied Science Research*, **2012**, 3 (4):2355-2368
- [21] Rami Reddy, G and Venkata Ramana, S.: *Advances in Appl. Sci. Research*, **2011**, 2(5), 240-248.
- [22] Rathod, V.P. and Channakote, M.M.: *Advances in Appl. Sci. Research*, **2011**, 2(3), 134-140.
- [23] Rathod, V.P. and Pallavi Kulkarni: *Advances in Appl. Sci. Research*, **2011**, 2(3), 265-279.
- [24] Ruksana Begum A, Narasimha Rao P and Prasada Rao, Non - Darcy Convective Heat Transfer in A Vertical Channel with Constant Heat Flux, *J. Pure & Appl. Phys.*, **Jan – Mar 2010**, 22, 1, 69-79.

- [25] Sreenadh, S, Nanda Kishore, S, Srinivas, A.N.S and Hemadri Reddy, R.: *Advances in Appl. Sci. Research*, **2011**, 2(6), 215-222.
- [26] Sudarsana Reddy P, Sreenivas G, Sreenivasa Rao P and Prasada Rao D R V, Non-darcy mixed convective heat and mass transfer flow of a viscous electrically conducting fluid through a porous medium in a circular annulus in the presence of temperature heat sources with Soret and Dufour effects-A Finite element Study, *Int.J.Comp &Appl.Maths*, **2010**, 5(5), 595-609.
- [27] Taneja, Rajeev and Jain N C, Effect of magnetic field on free convection mass transfer flow through porous medium with radiation and variable permeability in slip flow regime., *Janabha*, **2002**, 31/32, 69.
- [28] Tong T, Land Subramanian E, A boundary layer analysis for natural convection in porous enclosures: use of the Brinkman-extended Darcy model, *Int.J.Heat Mass Transfer*. **1985**, 28, 563-571.
- [29] Vafai K, Tien C L, Boundary and Inertia effects on flow and Heat Transfer in Porous Media, *Int. J. Heat Mass Transfer*, **1981**, 24, 195-203.
- [30] Vafai K, Thyagaraju, R, Analysis of flow and heat Transfer at the interface region of a porous medium, *Int. J. Heat Mass Trans.*, **1987**, 30, 1391-1405.